Journal of Applied Physics ARTICLE pubs.aip.org/aip/jap

Rectification of the alternating current using DW oscillations in magnetic nanostripes: Numerical simulation studies

Cite as: J. Appl. Phys. **139**, 073901 (2026); doi: 10.1063/5.0313174
Submitted: 20 November 2025 · Accepted: 27 January 2026 ·
Published Online: 17 February 2026

Dmitry Berkov[a] and Elena K. Semenova

AFFILIATIONS

General Numerics Research Lab, Kahlaische Str. 4, D-07745 Jena, Germany

[a]**Author to whom correspondence should be addressed:** d.berkov@general-numerics-rl.de

ABSTRACT

Energy of the ambient radio frequency electromagnetic field, which is always present due to the functioning of modern telecommunication devices, can be harvested by converting the ac-current—obtained from suitable antennas—into the dc-current employing a spin-torque diode (STD). Currently, this is a highly important topic by development of possible methods of the green energy production. In this paper, we present the optimal design of such an energy harvester basing on the oscillation of a domain wall (DW) inside a thin magnetic stripe with notches confining the displacement of this wall. First, we derive the maximal achievable conversion efficiency of a STD-based harvester. Afterward we show that among various designs of these devices, the highest efficiency (about 75% of the possible maximum) is obtained by using the oscillation of an out-of-plane DW confined in a stripe between two rectangular notches. Hence, we expect that this design open new perspectives for tunable spintronic rectifiers to be used as energy-harvesting elements in nanoscale devices.

I. INTRODUCTION

Radio frequency electromagnetic radiation is always available at least in the urban landscape due to different kinds of telecommunication systems—TV, mobile-phone networks, Wi-Fi devices, etc. Harvesting of the energy of this radiation is an important tasks of the applied physical research. Traditional technological solutions (e.g., Schottky diodes) of this problem (see, e.g., Refs. 1–3) are still not really satisfactory and, thus, other approaches are actively pursued.

In particular, a new concept for the microwave energy harvesting based on magnetic multilayer systems [mostly on magnetic tunnel junctions (MTJ)]—the concept of a spin-torque diode—was introduced in the pioneering paper.[4] In this paper, it was demonstrated that an *ac*-current through a multilayered nanopillar MTJ can produce a *dc*-voltage, which value is especially high if the current frequency coincides with the ferromagnetic resonance (FMR) frequency of the MTJ. This *ac* to *dc* conversion is based the spin-torque (ST) and magnetoresistance effects.[5,6] The ST from the ac-current induced the magnetization precession of the "free" magnetic layers of MTJ, and the resulting resistance oscillations of MTJ lead to a non-zero dc-voltage—see, e.g., Refs. 4 and 7–9. Corresponding energy harvesters would not be limited by the thermal voltage as other rectifier types mentioned above. Furthermore, MTJs can be incorporated into the existing CMOS technology without much efforts. A comprehensive review of this concept, its various implementations, and applications can be found in Ref. 10.

At present, mainly MTJ nanopillars are used for this purpose. In the so called resonant-type STDs, the magnetization of the free MTJ layer precesses around some in-plane direction due to the strong demagnetizing field within this layer (thin film nanoelement without a noticeable magnetocrystalline anisotropy). This behavior results in the resonant frequency dependence of the produced dc-voltage on the current frequency. Hence, the FMR frequency of the free layer should be adjusted to the frequency of the incident rf-radiation.[4,11–14]

Another STD type employs the out-of-plane magnetization precession (see, e.g., Refs. 7 and 15) which can be induced by a sufficiently strong out-of-plane magnetic anisotropy. This way a broad-band (non-resonant) energy harvesters may be obtained,

what is obviously an important advantage, because the spectrum of the ambient rf-radiation may possess significant peaks at many frequencies.

Recently, a hybrid design of an energy harvester was realized experimentally[16] and analyzed in detail theoretically[17] by connecting several in-plane resonant-type STDs with different resonant frequencies into an array. This design combines advantages of resonant-type STDs when compared to the non-resonant ones (higher sensitivity at their peak frequency and the absence of a finite threshold for the input rf-power for the dc-voltage generation)[7,15,18,19] with the feature of the broad-band rectification.

However, the rectification efficiency of all devices discussed above is still far below the theoretical limit, so the search for other possible designs of STD-based energy harvesters is at present an important topic in applications of the spin-torque effect.

In this paper, we analyze the perspectives to employ for the ac-current rectification oscillations of domain walls in magnetic nanostripes (flat nanowires), which can be used for this purpose in the same fashion as magnetic moment oscillations in MTJ nanopillars. Preliminary results in this direction have been obtained in Refs. 20–22. In Ref. 20, the DW was trapped at a random pinning site in the permalloy layer, and its high-frequency oscillations were excited demonstrating a very large DW velocity under these conditions and the generation of the rectified voltage. In other papers, a DW was stabilized in the free layer of a GMR stack due to its curved in-plane shape (arc-shape geometry) and the spin torque provided by a perpendicular-to-plane electric current was used to induce DW oscillations. The resulting rectified signal was used to make conclusions about the ST kind acting on these DWs (it was mainly the out-of-plane ST)[21] and to determine damping values for DW oscillations.[22]

In our research presented here, we study DW oscillations in thin nanostripes for both in-plane (IP) and out-of-plane (OOP, or perpendicular) DWs—see Fig. 1 for corresponding interval of the perpendicular magnetocrystalline anisotropy values—keeping

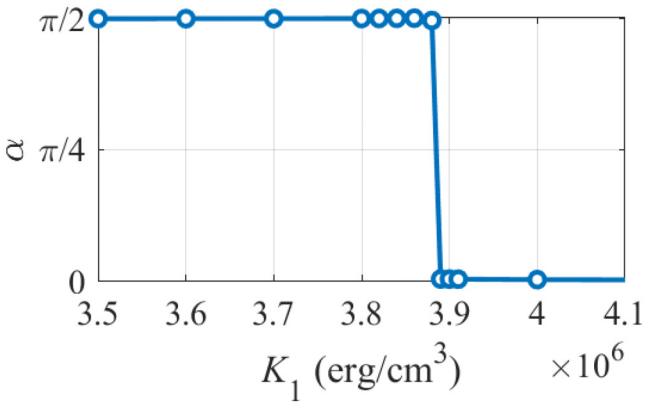

FIG. 1. Equilibrium angle α between the average magnetic moment **m** and out-of plane anisotropy axis **n** as a function of the out-of-plane anisotropy constant K_1 for the stripe with the thickness $h = 2$ nm and lateral sizes 400×100 nm^2; periodic boundary condition (PBC) in-plane were applied.

in mind the maximization of the current rectification efficiency for the STD effect. In contrast to already published geometries, we are going to stabilize the equilibrium DW position within the nanostripe using two notches on the opposite stripe edges. Varying the size and shape of these notches, we would be able not only to fix the equilibrium DW location (controlling the effective pinning field), but also to change the curvature of the energy landscape for a DW motion. Thus, we would be able to control both the basic oscillation frequency and oscillation amplitude of the DW for the given ac-current magnitude.

This paper is organized as follows. In Sec. II, we recall basic equations describing the voltage rectification magnetic multilayers due to the spin-torque effect (to make the paper self-contained). Furthermore, we introduce the reduced voltage which does not depend on ac-current amplitude and the zero-current resistance of the spin-torque diode and derive analytically the upper limit of this voltage. This limit allows us to compare the rectification efficiency of different STD designs. Main results are contained in Sec. III, where we discuss some general aspects of the DW dynamics in a stripe with notches (Subsection III A) and analyze the behavior of STDs based on the in-plane (Subsection III B) and out-of-plane (Subsection III C) domain walls. Final conclusion and some perspectives are presented in Sec. IV.

II. BASIC EQUATIONS AND DEFINITIONS

For our studies, we use the standard setup, where a harmonic spin-polarized ac-current (SPC) with the circular frequency ω_{ac} and the amplitude I_0 flows through a magnetic nanoelement in the direction perpendicular to the nanoelement plane (so called CPP-geometry),

$$I(t) = I_0 \cos(\omega_{ac} t) = I_0 \cdot i(t). \tag{1}$$

Resistance of this nanoelement becomes time-dependent due to the spin torque acting on the "free" magnetic layer and the giant (GMR) or tunnel (TMR) magnetoresistance effects,

$$R(t) = R_{\perp}^{(0)} r(t). \tag{2}$$

We consider the system where the TMR effect is used, so that

$$r(t) = \left\langle \frac{1}{1 + 0.5 \cdot \delta \cdot \cos\theta(t)} \right\rangle_{\{\mathbf{m}\}}. \tag{3}$$

In Eq. (2), $R_{\perp}^{0}$ denotes the resistance in the absence of any SPC, and δ in Eq. (3) is the material-dependent constant characterized the strength of the TMR effect. We simulate a simplified system, where we consider magnetization oscillations of the free layer only by the fixed polarization direction $\mathbf{S}_p$ of the incident current, so that $\theta(t)$ is the angle between the magnetizations of the "free" layer and $\mathbf{S}_p$.

The rectified voltage V_{dc} is then given by

$$V_{dc} = \langle I(t)R(t)\rangle_t = I_0 R_{\perp}^{(0)} \langle i(t)r(t)\rangle_t. \tag{4}$$

It is convenient to introduce the reduced dc-voltage,

$$\nu_{\rm dc} = \frac{V_{\rm dc}}{I_0 R_\perp^0} = \langle i(t) r(t) \rangle_t, \tag{5}$$

which is independent on the zero-current resistance and the ac-current amplitude and, thus, characterizes the efficiency of the suggested energy harvester design.

In particular, it is possible to derive the maximal possible value $\nu_{\rm dc}^{\rm max}$ of this reduced voltage. It would be achieved if the following conditions are met: (i) magnetization is always spatially homogeneous within the whole area flooded by the ac-current, (ii) magnetization projection on the current polarization direction oscillates with the maximal amplitude ($\Delta m_{\rm p} = 2$), and (iii) the phase shift between the oscillating magnetization and the ac-current is either zero or π. In this case, the averaging of (5) using the definitions (1) and (3) leads to the result,

$$\begin{aligned} \nu_{\rm dc}^{\rm max} &= \frac{1}{2\pi} \int_0^{2\pi} \frac{\cos x}{1 + 0.5 \cdot \delta \cos x} dx \\ &= \frac{2}{\delta} \left[1 - \left(1 - \frac{\delta^2}{4} \right)^{-1/2} \right] (\approx -\delta/4 \text{ for } \delta \ll 1). \end{aligned} \tag{6}$$

In this study, we use the value of $\delta = 0.9$, so that

$$\nu_{\rm dc} \approx -0.266. \tag{7}$$

For our simulations with employ the Landau–Lifshitz–Gilbert (LLG) equation,

$$\frac{d\mathbf{M}}{dt} = -\gamma_0 [\mathbf{M} \times \mathbf{H}] + \frac{\lambda}{M_{\rm s}} \left[\mathbf{M} \times \frac{d\mathbf{M}}{dt} \right] + T_{\rm ST} + T_{\rm FLT}, \tag{8}$$

with the Slonczewski spin torque,

$$\mathbf{T}_{\rm ST} = -\gamma_0 a_J [\mathbf{M} \times [\mathbf{M} \times \mathbf{S}_{\rm pol}]], \tag{9}$$

where a_J is given by

$$a_J = \frac{\hbar}{2|e|} \frac{J \cdot P}{M_{\rm s}^2 \cdot h}, \tag{10}$$

and a field-like torque terms,

$$\mathbf{T}_{\rm FLT} = -\gamma_0 b_J [\mathbf{M} \times \mathbf{S}_{\rm pol}], \tag{11}$$

where b_J is a field-like torque prefactor (see below). P in (10) denotes the current spin-polarization degree of the incident current and is set to $P = 0.6$.

Introducing the magnetization unit vector $\mathbf{m} = \mathbf{M}/M_s$, reduced field

$$\mathbf{h}_{\rm eff} = (\mathbf{H} + a_J [\mathbf{M} \times \mathbf{S}_{\rm pol}] + b_J \mathbf{S}_{\rm pol})/M_{\rm s} \tag{12}$$

and reduced time $\tau = t\gamma_0 M_{\rm s}$, we obtain Eq. (8) in reduced units,

$$\frac{d\mathbf{m}}{d\tau} = -[\mathbf{m} \times \mathbf{h}_{\rm eff}] - \lambda [\mathbf{m} \times [\mathbf{m} \times \mathbf{h}_{\rm eff}]]. \tag{13}$$

Finally, we define the factor $c_{\rm fl}$ as proportionally coefficient between b_J and a_J as $b_J = c_{\rm fl} a_J$ and set $c_{\rm fl} = 0.4$ (see Ref. 21).

For solving the LLG equation, we have used our MicroMagus package with the adaptive step-size control for dynamic simulations.[23] Thermal fluctuations were not taken into account ($T = 0$).

For our considerations, we also need the oscillation amplitude A_α ($\alpha = x, y, z$) of the corresponding magnetization component, which for sinusoidal signal is defined as

$$A_\alpha = \frac{1}{2} (\max(m_\alpha(t)) - \min(m_\alpha(t))) \tag{14}$$

for a non-sinusoidal signal as

$$A_\alpha = \sqrt{2 \langle \tilde{m}_\alpha{}^2(t) \rangle}, \tag{15}$$

where

$$\tilde{m}_\alpha(t) = m_\alpha(t) - \langle m_\alpha(t) \rangle. \tag{16}$$

Phase shift between the current and magnetization component for a sin-like signal is

$$\Delta\phi = \arccos(2 \langle \tilde{J}(t) \tilde{m}_z(t) \rangle), \tag{17}$$

where $\tilde{J}(t) = J(t)/J_0$, and for a non-sinusoidal signal can be evaluated as

$$\Delta\phi = \arccos\left(\frac{2}{A_z} \langle \tilde{J}(t) \tilde{m}_z(t) \rangle \right). \tag{18}$$

III. DC-VOLTAGE FOR DW OSCILLATIONS IN A THIN MAGNETIC STRIPE

A. DW dynamics in a stripe with notches: General consideration

As pointed out in Sec. I, we consider an energy harvester design based on the DW oscillations in a thin magnetic nanostripe. Two notches are placed on both sides of this stripe to create an energy minimum for the DW, which oscillations around this minimum due to the SPC lead to the current rectification.

The corresponding geometry is shown in Fig. 2. We simulate a magnetic stripe with in-plane dimensions $600 \times 100\,\text{nm}^2$, thickness $h = 2\,\text{nm}$, and two rectangular edge notches, each of width 50 nm and depth 10 nm. The in-plane discretization uses square cells of $2.5 \times 2.5\,\text{nm}^2$. Material parameters are the saturation magnetization $M_s = 800\,\text{G}$ and the exchange stiffness $A = 10^{-6}\,\text{erg/cm}$. The magnetocrystalline anisotropy axis is oriented along the film normal, $\mathbf{n} = (0, 0, 1)$, i.e., perpendicular to the stripe plane. The spin-polarized current flows only through the

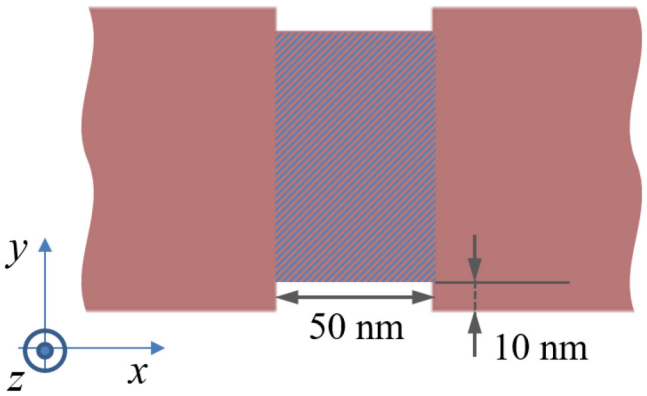

FIG. 2. In-plane shape of the simulated stripe with two rectangular notches each having the width 50 nm and depth 10 nm. Current flows only through the shaded area.

stripe segment confined between the notches (shaded area in Fig. 2).

The geometry of a stripe with rectangular notches is introduced to realize a nearly flat energy landscape for a domain wall (DW) within the window defined by these notches. As long as the DW center remains between the notch ends, the restoring force is weak and no well-defined small-amplitude eigenfrequency emerges. Consequently, a resonance in the usual sense is not expected: the relevant time scale is governed "kinematically" by the motion of the DW between the two notch ends rather than by some harmonic modes in a well-defined energy minimum (as, e.g., for semicircular or triangular notches like those used in Ref. 24, where the possibility of designing spin-torque resonators using DW oscillations was suggested). In this situation, the maximum of the frequency dependence of the dc-voltage is anticipated when the frequency of the spin-polarized current matches the DW traveling time between the notch boundaries within a half-period of the current oscillations, i.e., when the wall reliably reaches a barrier near current extrema.

We note that our setup is very different from the standard situation in many systems, where the understanding of the interplay between the DW width and the notch dimensions is an important ingredient for the analysis of the DW dynamics. In our work, however, the rectangular-notch geometry creates an almost flat energy landscape for the DW between the notch edges, so that there is no well-defined localized pinning potential in the usual sense. For these reasons, the classical dependence of the pinning strength on the ratio of the DW width to the notch size does not influence the physical mechanism we study—namely, the kinematic synchronization responsible for the rectification maximum. Hence, we did not perform the analysis of this dependence.

Domains on opposite sides of the notches have opposite magnetization orientations. Hence, we expect that the corresponding dc-voltage may almost achieve its maximal value (6), because the amplitude of magnetization oscillation within the area between the two notches can be nearly maximal ($\Delta m_{x(z)} \approx 2$).

To span the two symmetry classes of interest, we consider both in-plane (IP) and out-of-plane (OOP) domain walls. Equilibrium DW configurations for the two parameter sets are shown in Fig. 3. For the IP wall, we use $K_1 = 3.5 \times 10^6$ erg/cm^3; for the OOP wall, we use $K_1 = 4.0 \times 10^6$ erg/cm^3. In each case, the spin-polarization vector is chosen parallel to the equilibrium magnetization of the adjacent domains in order to favor controlled translational motion along the stripe: $\mathbf{S}_p = (1, 0, 0)$ for the IP domains and $\mathbf{S}_p = (0, 0, 1)$ for the OOP domains. For this choice of $\mathbf{S}_p$, the spin torque acts effectively like an oscillating magnetic field applied along the same direction, promoting a well-controlled shift of the DW along the stripe and thereby maximizing the amplitude of magnetization oscillations within the readout window.

In Secs. III B and III C, we analyze the magnetization dynamics and rectified response for the IP and OOP walls under these conditions, using the same notch geometry and current confinement to enable a direct comparison.

B. DC-voltage generated by an in-plane DW

To obtain a well-defined in-plane domain wall (DW), the perpendicular anisotropy constant was set to $K_1 = 3.5 \times 10^6$ erg/cm^3. Under these conditions, the equilibrium configuration corresponds to a Néel-like wall lying in the stripe plane, as illustrated in Fig. 3(a).

The spin-polarized current with polarization vector $\mathbf{S}_p = (1, 0, 0)$ was injected perpendicular to the stripe. For this configuration, the combined action of the Slonczewski and field-like spin-transfer torques, together with the Gilbert damping term in the Landau–Lifshitz–Gilbert (LLG) equation, produces a translational motion of the DW along the stripe axis, i.e., along the corridor confined by the two rectangular notches.

The time evolution of the in-plane magnetization component $m_x(t)$, averaged over the current-carrying window, is shown in Fig. 4 together with the driving ac-current for two representative current frequencies. This component directly reflects the position of the wall: when the DW is near one end of the window, m_x takes one extreme value, and when it reaches the opposite end, m_x reverses sign.

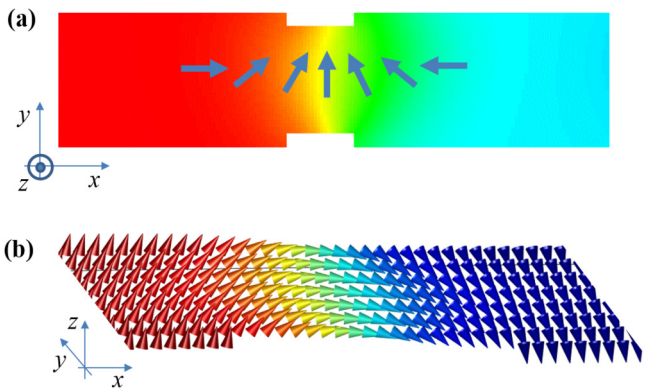

FIG. 3. Equilibrium magnetization configurations for the in-plane (a) and out-of-plane (b) domain walls.

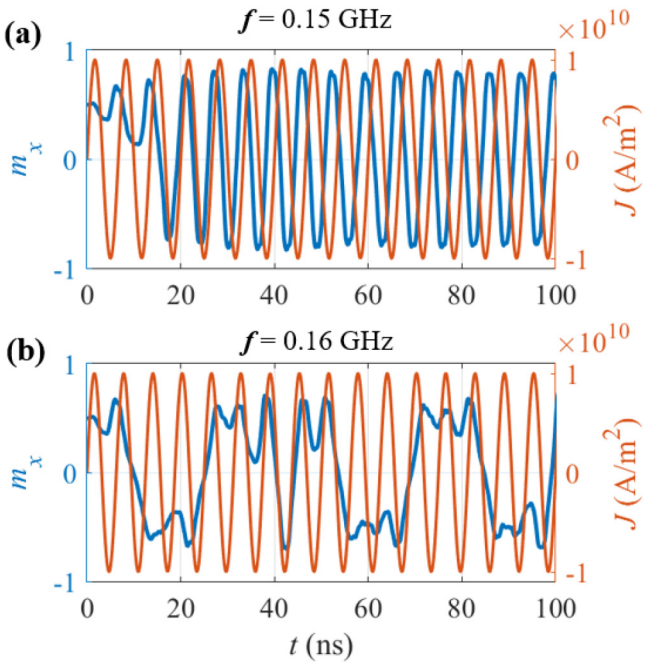

FIG. 4. In-plane DW [$K_1 = 3.5 \times 10^6$ erg/cm^3, $S_p = (1, 0, 0)$]: m_x-oscillations in the rectangular-notch region on the stripe with for the current density amplitude $J_0 = 1 \times 10^{10}$ A/m^2 and frequencies $f = 0.15$ GHz (a) and $f = 0.16$ GHz (b).

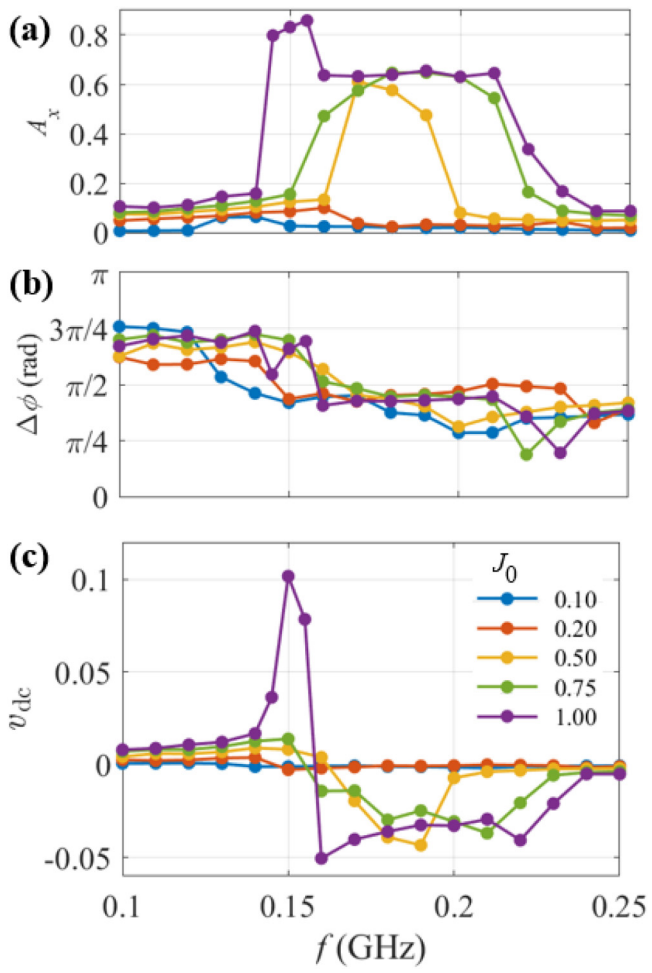

FIG. 5. Cumulative results for the in-plane DW [$K_1 = 3.5 \times 10^6$ erg/cm^3, $S_p = (1, 0, 0)$]. Amplitude A_x of the m_x-oscillations in the area between the notches (a), phase shift $\Delta\phi$ between the current and m_x-oscillations and the dc-voltage (b) as functions of the ac-current frequency for different current amplitudes J_0 ($\times 10^{10}$A/m^2), indicated in the legend on the panel (c).

For the current frequency $f = 0.15$ GHz [Fig. 4(a)], time of the domain wall motion between the notch ends corresponds exactly to one half of the ac-current period. Hence, DW oscillates between the two limiting positions corresponding to the two ends of the stripe region between notches. Thus, we achieve the nearly maximal oscillation amplitude of m_x within the notch area.

When the current frequency is slightly increased to $f = 0.16$ GHz, the polarity of the driving current reverses faster than the wall can complete its transit between the notch ends. Consequently, the DW motion becomes out of phase with the current oscillation: the wall begins to reverse its direction of motion before reaching the opposite notch edges. Thus, it becomes partially localized near one edge of the area between the notches during several current cycles, oscillating around a limited region instead of traversing the full distance. The variation of the m_x-component is, therefore, strongly reduced, and the magnetization waveform becomes distorted relative to the sinusoidal drive. This reduction of the oscillation amplitude of m_x leads directly to a decrease of the rectified voltage.

Cumulative results for the in-plane DW are displayed in Fig. 5, where frequency dependencies of the m_x-oscillations amplitude A_x within the notch area [panel (a)], phase shift between the current and m_x-oscillations (b), and the reduced voltage (c) are shown.

Comparing these frequency dependencies, we can see that largest positive and negative values of the dc-voltage are obtained for frequencies where (i) A_x are large and (ii) the phase shift between magnetization and current is considerably different from $\pi/2$.

The frequency $f = 0.15$ GHz represents the optimal condition for the chosen stripe geometry and material parameters. Here, the DW motion is coherent and the wall position closely tracks the ac drive, leading to strong oscillations of the average magnetization betwen the notches. Nevertheless, even in this favorable regime, the absolute value of the reduced dc-voltage $v_{dc} \approx 0.1$ remains significantly smaller than the theoretical limit $v_{dc}^{max} \approx 0.27$ (7) derived for the spatially uniform precession. The reason for this discrepancy lies in the phase delay between the DW motion and the driving current: although the amplitude of the magnetization oscillation reaches $A_x \approx 0.85$, the phase shift never approaches the "good"

values $\Delta\varphi = 0$ or π that would yield the maximal rectification. Instead, the DW dynamics introduces a finite delay due to damping term, so that the voltage remains well below the theoretical upper bound.

In summary, the in-plane DW exhibits a clear kinematic resonance corresponding to the condition when the DW traverses the notch corridor within half of the ac-current period. At this frequency, the oscillation amplitude of the in-plane magnetization is nearly maximal, and the resulting rectified voltage attains its highest absolute value. A further increase in frequency leads to loss of synchronization between current and DW motion, reduction of A_x, and the phase shift between the current and magnetization $\Delta\phi \approx \pi/2$, thus leading to the rapid fall of v_{dc}. Our results show that for the in-plane wall, the efficiency of current rectification is primarily limited not by the amplitude of the DW motion, but by the unfavorable phase shift between the driving current and the magnetization response. Section III C will show that the situation differs markedly for the out-of-plane wall, where the achievable amplitude itself becomes the key constraint.

C. DC-voltage generated by an out-of-plane DW

To obtain a well-defined out-of-plane (OOP) domain wall (DW), the perpendicular anisotropy constant was increased to $K_1 = 4.0 \times 10^6$ erg/cm^3. This value substantially exceeds the critical threshold separating the in-plane and out-of-plane regimes and ensures that the magnetization within the domains is oriented predominantly along the normal to the film. The spin-polarization vector was chosen as $\mathbf{S}_p = (0, 0, 1)$, i.e., parallel to the equilibrium magnetization of the domains. Under these conditions, the action of the spin-transfer torques and damping drives the wall along the stripe axis, similar to the in-plane case, but now the oscillation involves mainly the out-of-plane magnetization component m_z.

The equilibrium configuration of the domains and the DW for this parameter set is shown in Fig. 3(b). Because the strong out-of-plane magnetocrystalline anisotropy partially compensates the in-plane shape anisotropy of the stripe, the wall is not of the ideal Bloch–Landau type. Instead, the magnetic moments rotate predominantly in the xz-plane, giving the wall a mixed Bloch–Néel character. This configuration remains stable in zero current and provides a well-defined starting state for dynamic simulations.

The typical temporal evolution of the OOP wall is illustrated in Fig. 6. Panel (a) displays the time dependence of the averaged out-of-plane magnetization component $\langle m_z(t)\rangle$ in the current-carrying window together with the applied ac current. Panel (b) shows the snapshots of the magnetization distribution within and around the notch region for during one oscillation cycle.

For the ac-current frequency $f = 0.17$ GHz chosen for this example, the wall oscillates coherently between the two limiting positions defined by the notch edges. The travel time of the DW between these two boundaries matches almost exactly one half of the ac-current period. As a consequence, the average magnetization in the window alternates between its extreme values, and the change of $\langle m_z\rangle$ approaches its theoretical maximum $\Delta m_z = 2$. This regime corresponds to the optimal kinematic synchronization of the OOP wall with the external drive.

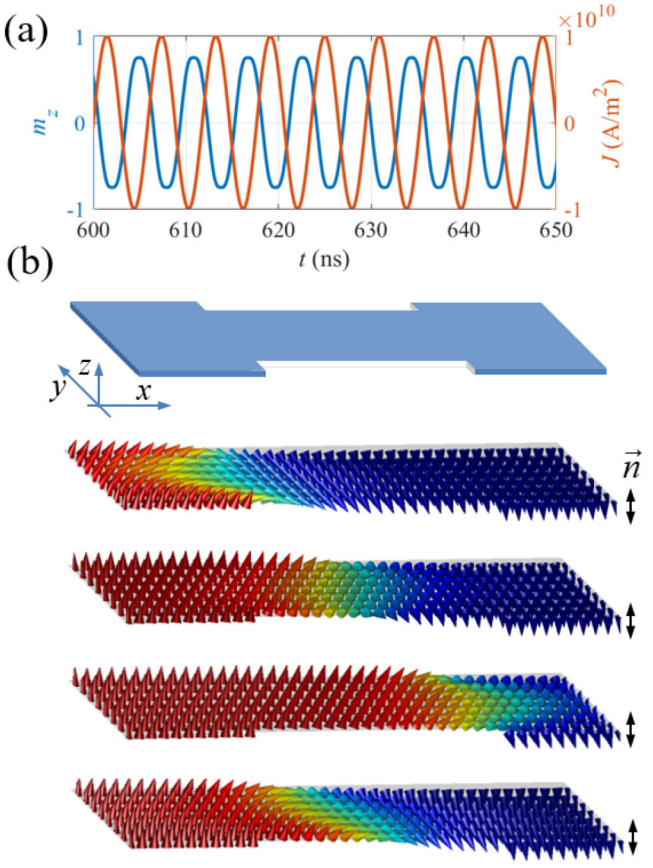

FIG. 6. Dynamics of magnetization oscillation in the out-of-plane DW: (a) $\langle m_z(t)\rangle$ averaged over the rectangular-notch region and (b) 3D snapshots of the DW configurations. Amplitude of the ac-current oscillations $J_0 = 1 \times 10^{10}$ A/m^2 and oscillation frequency $f = 0.17$ GHz.

Cumulative results summarizing the OOP-DW dynamics are presented in Fig. 7. The three panels show, respectively: (a) the frequency dependence of the oscillation amplitude A_z of $\langle m_z\rangle$ within the notch region, (b) the phase shift $\Delta\varphi$ between the current and magnetization oscillations, and (c) the resulting reduced dc-voltage v_{dc}.

The trends resemble those obtained for the in-plane wall but exhibit several notable differences. The most pronounced positive and negative dc-voltage values are observed at frequencies for which the oscillation amplitude A_z is large and the phase shift between $m_z(t)$ and the current is close to either 0 or π. In the first case, the magnetization and current vary nearly in phase, producing a positive rectified voltage; in the latter, the oscillations are out of phase by π, resulting in a voltage of opposite sign.

The overall frequency dependence of v_{dc} exhibits a broad maximum centered near $f = 0.16 - 0.17$ GHz, in good agreement with the kinematic expectation that optimal rectification occurs when the DW completes one full back-and-forth motion during a single ac-current period.

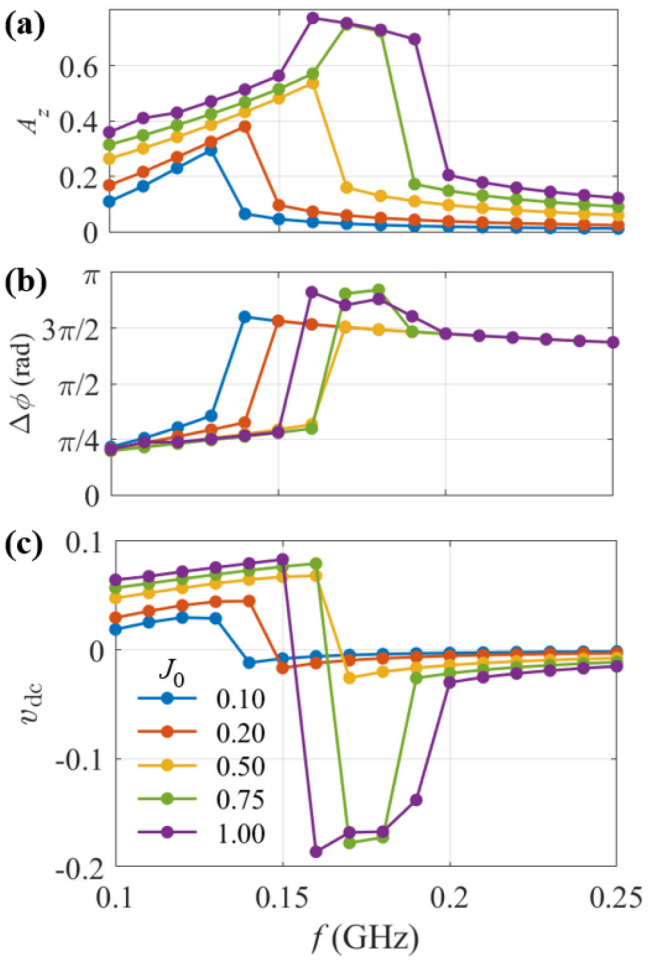

FIG. 7. Out-of plane DW dynamics for different amplitudes of the ac-current density J_0 as indicated in the legend: (a) amplitude of the magnetization oscillations of $\langle m_z \rangle$ as a function of frequency; (b) phase shift between the current and magnetization oscillations; and (c) reduced voltage.

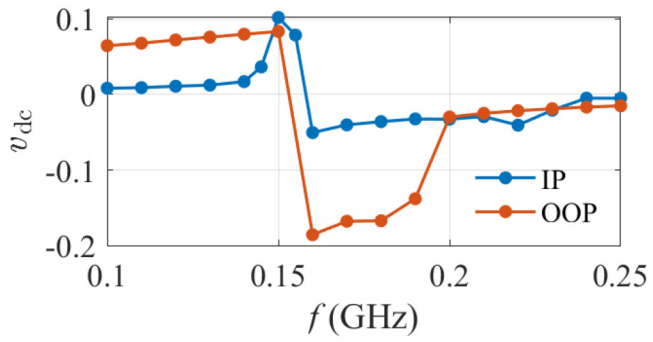

FIG. 8. Voltage as a function of frequency for two types of DW: in-plane DW for $K_1 = 3.5 \times 10^6$ erg/cm^3 and $S_p = (1, 0, 0)$ (blue line) and out-of-plane DW for $K_1 = 4.0 \times 10^6$ erg/cm^3 and and $S_p = (0, 0, 1)$ (red line). Current density amplitude is $J_0 = 1 \times 10^{10}$ A/m^2.

The maximal absolute value of the dc-voltage (observed at $f = 0.16$ GHz) $|v_{dc}| \approx 0.2$ is two times higher than for the in-palne DW, but still does not achieve the possible maximum $|v_{dc}| \approx 0.27$ given by (6). The main factor limiting the dc-voltage in this setup is the amplitude of magnetization oscillations, since the factor arising from the phase shift is very close to unity: $\cos(\Delta\phi) \approx 0.97$ at this frequency. Even at the optimal frequency, the spatially averaged amplitude of $\langle m_z \rangle$ oscillations reaches only about $A_z \approx 0.8$.

This reduction is due to the internal non-uniformity of the magnetization near the DW center, where the rotation of moments in the xz-plane prevents complete saturation of m_z in either direction. In other words, although the wall moves through almost the entire width of the notch region, the local magnetization near its core remains tilted, and the averaged m_z never attains the fully saturated values corresponding to ± 1. As a result, the modulation of the magnetoresistive signal is somewhat smaller than the idealized two-domain model would predict, leading to a reduced v_{dc}.

Hence, further enhancement of v_{dc} would require increasing the magnetization oscillation amplitude either by modifying the notch geometry to allow a slightly larger DW displacement or by fine-tuning the anisotropy and damping parameters to make the wall narrower.

Overall, the out-of-plane wall demonstrates a more favorable dynamical behavior for current rectification compared to the in-plane wall, as shown in Fig. 8. The oscillation of the average magnetization component remains highly coherent over a broad frequency range, and the phase relation with the drive is nearly ideal. The main constraint on performance stems from the incomplete reversal of the magnetization rather than from the temporal desynchronization. Consequently, while the achievable v_{dc} remains below its theoretical limit, the out-of-plane DW configuration provides a robust and efficient rectification mechanism that is less sensitive to the precise driving frequency.

We close this section with a brief explanation of the difference between the in-plane and out-of-plane concerning the phase coherence during thie motion. The most probable explanation of this difference is as follows. In the OOP configuration, the magnetization dynamics is essentially uniaxial, and the spin-transfer torque acts almost exactly along the preferred axis. As a result, the OOP-DW tends to move in a nearly simple translational manner with very little internal rotation, which minimizes the phase lag with respect to the driving current. By contrast, the in-plane DW must accommodate additional tilting and internal deformation due to demagnetizing fields during its motion, which introduces a noticeable inherent delay even when the oscillation amplitude is large.

IV. CONCLUSION

In this study, we have investigated two setups of a spin-torque energy harvester based on the current-driven domain wall motion in a thin ferromagnetic nanostripe with two rectangular notches at the opposite edges. Using micromagnetic simulations, we analyzed the dynamic response of both in-plane and out-of-plane walls

under an alternating spin-polarized current and identified the key parameters that determine the rectification efficiency.

The most efficient device design was found to consist of a stripe with two rectangular notches (whose width is much smaller than the overall stripe length) and magnetic parameters ensuring the out-of-plane magnetization of a stripe in equilibrium. This geometry creates an effective potential landscape that is nearly flat within the region between the notch terminations, with sharp barriers at the notch ends. Owing to this feature, the DW can move almost freely within the central corridor, so that it can be shifted with relatively small amplitudes of the driving ac-current. Unlike systems with parabolic energy confinement, where a well-defined resonance frequency exists, the rectangular-notch configuration exhibits kinematic synchronization: the optimal response occurs for the ac-current frequency when the DW traverses the corridor once during a half-period of the current oscillation.

In this geometry, magnetization direction within the stripe region between the notches oscillates with almost maximal possible amplitude ($\Delta m_\alpha \approx 2$, or $A_\alpha \approx 1$), resulting in the generation of the dc-voltage close to its maximal possible value given by expression (6).

Overall, the rectangular-notch geometry provides a simple and robust route toward efficient spin-torque energy harvesting. Its nearly flat potential landscape allows coherent, large-amplitude DW oscillations at moderate current densities and without a precise frequency tuning (for the out-of-plane DW).

Within this simple model, additional optimization of the notch dimensions and magnetic material parameters can further enhance the output voltage and power conversion efficiency. In future, systematic studies of the more realistic models of multilayered stripes, including the magnetodipolar interaction and possibly the Dzyaloshinskii–Moriya interaction (in systems with the appropriate symmetry properties) between magnetic layers could be performed. Prediction resulting from these simulations will pave the way for compact, tunable spintronic rectifiers and energy-harvesting elements integrated into nanoscale devices.

ACKNOWLEDGMENTS

Financial support of the Deutsche Forschungsgemeinschaft (German Research Society), DFG-Project No. BE 2464/21-1 is greatly acknowledged.

AUTHOR DECLARATIONS

Conflict of Interest

The authors have no conflicts to disclose.

Author Contributions

Dmitry Berkov: Conceptualization (lead); Funding acquisition (equal); Investigation (supporting); Methodology (equal); Project administration (lead); Software (equal); Supervision (lead); Validation (equal); Writing – original draft (equal). **Elena K. Semenova:** Formal analysis (equal); Investigation (equal); Methodology (supporting); Software (equal); Validation (equal); Visualization (lead); Writing – review & editing (equal).

DATA AVAILABILITY

The data that support the findings of this study are available from the corresponding author upon reasonable request.

REFERENCES

[1]S. Hemour and K. Wu, Proc. IEEE **102**, 1667 (2014).
[2]S. Hemour, Y. Zhao, C. H. P. Lorenz, D. Houssameddine, Y. Gui, C.-M. Hu, and K. Wu, IEEE Trans. Microwave Theory Tech. **62**, 965 (2014).
[3]M. Cansiz, D. Altinel, and G. K. Kurt, Energy **174**, 292 (2019).
[4]A. A. Tulapurkar, Y. Suzuki, A. Fukushima, H. Kubota, H. Maehara, K. Tsunekawa, D. D. Djayaprawira, N. Watanabe, and S. Yuasa, Nature **438**, 339 (2005).
[5]J. C. Slonczewski, J. Magn. Magn. Mater. **159**, L1 (1996).
[6]D. C. Ralph and M. D. Stiles, J. Magn. Magn. Mater. **320**, 1190 (2008).
[7]O. V. Prokopenko, I. N. Krivorotov, E. Bankowski, T. Meitzler, S. Jaroch, V. S. Tiberkevich, and A. N. Slavin, J. Appl. Phys. **111**, 123904 (2012).
[8]S. Miwa, S. Ishibashi, H. Tomita, T. Nozaki, E. Tamura, K. Ando, N. Mizuochi, T. Saruya, H. Kubota, K. Yakushiji, T. Taniguchi, H. Imamura, A. Fukushima, S. Yuasa, and Y. Suzuki, Nat. Mater. **13**, 50 (2014).
[9]E. Kowalska, A. Fukushima, V. Sluka, C. Fowley, A. Kákay, Y. Aleksandrov, J. Lindner, J. Fassbender, S. Yuasa, and A. M. Deac, Sci. Rep. **9**, 9541 (2019).
[10]M. Harder, Y. Gui, and C.-M. Hu, Phys. Rep. **661**, 1 (2016).
[11]C. Wang, Y.-T. Cui, J. Z. Sun, J. A. Katine, R. A. Buhrman, and D. C. Ralph, Phys. Rev. B **79**, 224416 (2009).
[12]G. Finocchio, M. Ricci, R. Tomasello, A. Giordano, M. Lanuzza, V. Puliafito, P. Burrascano, B. Azzerboni, and M. Carpentieri, Appl. Phys. Lett. **107**, 262401 (2015).
[13]B. Fang, M. Carpentieri, X. Hao, H. Jiang, J. A. Katine, I. N. Krivorotov, B. Ocker, J. Langer, K. L. Wang, B. Zhang, B. Azzerboni, P. K. Amiri, G. Finocchio, and Z. Zeng, Nat. Commun. **7**, 11259 (2016).
[14]L. Zhang, B. Fang, J. Cai, M. Carpentieri, V. Puliafito, F. Garescì, P. K. Amiri, G. Finocchio, and Z. Zeng, Appl. Phys. Lett. **113**, 102401 (2018).
[15]R. Tomasello, B. Fang, P. Artemchuk, M. Carpentieri, L. Fasano, A. Giordano, O. Prokopenko, Z. Zeng, and G. Finocchio, Phys. Rev. Appl. **14**, 024043 (2020).
[16]R. Sharma, T. Ngo, E. Raimondo, A. Giordano, J. Igarashi, B. Jinnai, S. Zhao, J. Lei, Y.-X. Guo, G. Finocchio, S. Fukami, H. Ohno, and H. Yang, Nat. Electron. **7**, 653 (2024).
[17]E. K. Semenova and D. Berkov, J. Appl. Phys. **136**, 083907 (2024).
[18]P. N. Skirdkov and K. A. Zvezdin, Ann. Phys. **532**, 1900460 (2020).
[19]L. Zhang, H. Tu, Y. Luo, K. Zeng, X. Tao, D. Zhao, B. Fang, and Z. Zeng, Appl. Phys. Lett. **122**, 092405 (2023).
[20]C. T. Boone, J. A. Katine, M. Carey, J. R. Childress, X. Cheng, and I. N. Krivorotov, Phys. Rev. Lett. **104**, 097203 (2010).
[21]A. Chanthbouala, R. Matsumoto, J. Grollier, V. Cros, A. Anane, A. Fert, A. V. Khvalkovskiy, K. A. Zvezdin, K. Nishimura, Y. Nagamine, H. Maehara, K. Tsunekawa, A. Fukushima, and S. Yuasa, Nat. Phys. **7**, 626 (2011).
[22]S. Lequeux, J. Sampaio, P. Bortolotti, T. Devolder, R. Matsumoto, K. Yakushiji, H. Kubota, A. Fukushima, S. Yuasa, K. Nishimura, Y. Nagamine, K. Tsunekawa, V. Cros, and J. Grollier, Appl. Phys. Lett. **107**, 182404 (2015).
[23]D. V. Berkov and N. L. Gorn, see http://www.micromagus.de for "Micromagus: Package for Micromagnetic Simulations" (2024).
[24]S. Lepadatu, O. Wessely, A. Vanhaverbeke, R. Allenspach, A. Potenza, H. Marchetto, T. R. Charlton, S. Langridge, S. S. Dhesi, and C. H. Marrows, Phys. Rev. B **81**, 060402 (2010).